Savin H, Repo P, von Gastrow G, Ortega P, Calle E, Garin M, Alcubilla R. Black silicon solar cells with interdigitated back-contacts achieve 22.1% efficiency. Nature nanotechnology. 2015 May 18.

Postprint manuscript for self-archiving purposes.
Nature Nanotechnology (2015) doi:10.1038/nnano.2015.89
http://www.nature.com/nnano/journal/vaop/ncurrent/full/nnano.2015.89.html

Black silicon solar cells with interdigitated back-contacts achieve 22.1% efficiency

Hele Savin[1,*], Päivikki Repo[1], Guillaume von Gastrow[1], Pablo Ortega[2], Eric Calle[2], Moises Garín[2] and Ramon Alcubilla[2]

[1] Aalto University, Department of Micro and Nanosciences, Tietotie 3, 02150 Espoo, Finland

[2] Departament d'Enginyeria Electrònica, Universitat Politècnica de Catalunya, Jordi Girona 1-3, Mòdul C4, 08034 Barcelona, Spain

*corresponding author: hele.savin@aalto.fi

Abstract

The nanostructuring of silicon surfaces – known as black silicon – is a promising approach to eliminate front-surface reflection in photovoltaic devices without the need for a conventional antireflection coating. This might lead to both an increase in efficiency and a reduction in the manufacturing costs of solar cells. However, all previous attempts of integrating black silicon into solar cells have resulted in cell efficiencies much below 20% due to the increased charge carrier recombination at the nanostructured surface. Here we show that a conformal alumina film can solve the issue of surface recombination in black silicon solar cells by providing chemical and electrical passivation. We demonstrate that efficiencies above 22% can be reached, even in thick interdigitated back-contacted cells, where carrier transport is very sensitive to front surface passivation. This means that the surface recombination issue has truly been solved and black silicon solar cells have a real potential to industrial production. Furthermore, we show that use of black silicon can result in 3% increase in the daily energy production when compared to a reference cell with the same efficiency, due to its better angular acceptance.

Introduction

Black-silicon (b-Si) – as its name implies – absorbs light very efficiently in a wide range of wavelengths and as a result appears black to the naked eye. High absorption is based on gradual matching of the refractive index at the silicon-air interface using small nanostructures with dimensions below the wavelength of the incident light[1]. Various shapes, such as nanocones[2], nanowires[3], microwires[4] and porous silicon[5], have been used for achieving excellent light management effects. Because of its many superior properties, b-Si has potential for a range of applications such as self-cleaning surfaces[6], microelectromechanical systems[7], ion mobility spectrometers[8], terahertz emitters[9], drug analysis[10], photodetectors[11] and antibacterial surfaces[12].

Black silicon would also appear to be an ideal material for photovoltaics due to its outstanding light management properties under the solar spectrum. In addition to boosting the efficiency, b-Si can result in significant savings in the manufacturing costs as there is no need to deposit a separate antireflection coating. The main challenges that have hindered the use of b-Si in photovoltaics are related to the increased surface recombination due to the larger surface area of the nanostructures; the situation is even more challenging in conventional front-contacted solar cell structure due to Auger recombination at the highly-doped nanostructures[5]. This means that a high amount of light-generated electron-hole pairs is lost in the nanostructures instead of being collected at the contacts, reducing the efficiency. Auger recombination can be avoided by using an Interdigitated Back Contact (IBC) solar cell design where the junction and the contacts are placed at the back of the cell[13], but the recombination problem due to the larger surface area remains unsolved. So far, the surface passivation issue has been generally addressed by rather conventional methods such as silicon nitride deposited by plasma enhanced chemical vapour deposition[14] or thermally grown silicon dioxide[15], resulting in tradeoffs between reflectance and recombination. Therefore, the final efficiency has been limited by the recombination at the increased b-Si surface and the reported efficiencies have remained well below 20% (18.2% with a surface area of 0.8 cm^2)[5]. However, our preliminary experiments on pin-hole free and highly conformal atomic layer deposited (ALD) thin films combined with the chemical and field effect passivation ability of Al_2O_3[16] have shown promising results to overcome the problematic surface recombination issue in black silicon[17]. Minority carrier lifetimes in the millisecond range indicate excellent surface passivation of b-Si and are in the range needed for high efficiency solar cells (> 20 %)[17, 18].

Previous black silicon solar cell results have been limited to conventional front-side aluminium back surface field (Al-BSF) structures or ultrathin back-contacted cells[13], probably because these structures are less sensitive to front surface recombination. Here we study the potential of the ALD Al_2O_3 passivated black silicon to address the above mentioned surface recombination problem present in nanostructured surfaces. Thereby we select a solar cell design that is known to be extremely sensitive to surface recombination, *i.e.* thick

interdigitated back-contact back-junction (IBC) solar cell[19]. In IBC cells, a majority of the photogenerated charge carriers need to diffuse a long distance from the front surface to the backside of the cells. Thick IBC cell is thus a very demanding structure even for conventionally textured solar cells. The goal here is to demonstrate that, if black silicon works in this highly demanding structure, then the surface recombination challenge can be considered solved and black silicon should be applicable to other cell structures as well.

Reflectance and surface recombination

Different methods for fabricating black silicon have been introduced such as laser texturization[20], plasma immersion ion implantation[14] or metal-assisted wet etching[21]. Here, we use cryogenic deep reactive ion etching (DRIE) as it has multiple advantages: it is fast and inexpensive and there is no dependence on the crystalline orientation nor need for mask layers[22]. As can be seen from Fig. 1a, etching results in random nanoscale structures with a typical height of around 800 nm and width of 200 nm. Precise description of the black silicon fabrication is given in the Methods section. In principle, however, the results presented here should be independent on the b-Si fabrication method.

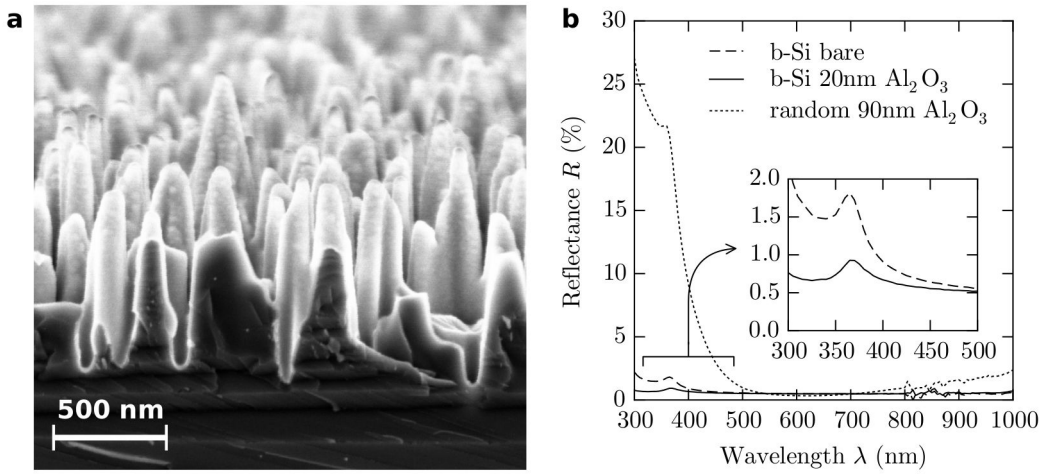

Figure 1. Structure and the reflectance of black silicon. a) Scanning electron microscopy (SEM) image, cross-sectional view, of a b-Si surface. Typical height of a silicon pillar is around 800 nm and diameter from the bottom of the pillar around 200 nm. The 20 nm Al_2O_3 layer can be seen as a brighter layer on top of the pillars. b) Measured reflectance spectra in the 300-1000 nm wavelength range. The dashed line represents the reflectance of a bare b-Si sample whereas the black solid line represents the reflectance of b-Si with 20 nm of Al_2O_3 (zoomed image shown in the inset). The reflectance of random pyramids coated with 90 nm thick Al_2O_3 film, dotted line, is shown as a reference.

In order to passivate black silicon we deposited a thin, 20 nm, Al_2O_3 film as described in the Methods section. As a reference, we prepared samples with conventional micrometre scale random pyramids and a 90 nm thick Al_2O_3 antireflection (AR) coating. Fig. 1b shows the measured reflectance of a b-Si wafer with and without the passivation film. Although extremely low reflectance is already reached with the bare b-Si surface, the Al_2O_3 layer further reduces the reflectance to less than 1% between 300-1000 nm (see the figure inset), which is the relevant wavelength range for solar cells. When compared to the random pyramid reference with a thick AR film, the benefit of b-Si becomes clear as in this material the reflectance is much lower in the short (300-500 nm) and long (>700 nm) wavelengths. Moreover, it is well known that the positive impact of b-Si further increases when the light enters the cell from a wider angle[23]. The impact of the angle of incidence on the solar cell efficiency will be shown later in the paper.

Minority carrier lifetime is a material quality dependent parameter indicative of the time that it takes for the photogenerated charge carriers to recombine. It is a direct indicator of the maximum efficiency a solar cell can reach – the higher the lifetime the higher the cell efficiency. Lifetime measurements give as a result an effective carrier lifetime τ_{eff}, which is affected not only by the lifetime at the bulk but also by the recombination at the wafer surfaces. Thus, it gives an idea about how well the surfaces are passivated. A direct indicator of the surface passivation quality is the surface recombination velocity S_{eff} that describes the velocity at which charge carriers reach the surface to recombine. When both surfaces are identical, the surface recombination velocity is related to the effective minority carrier lifetime through:

$$S_{eff} = \frac{W}{2}\left(\frac{1}{\tau_{eff}} - \frac{1}{\tau_{in}}\right) \quad (1)$$

where W is the wafer thickness, τ_{eff} the measured effective carrier lifetime and τ_{in} the intrinsic carrier lifetime according to parametrization by Richter et al.[24] As mentioned earlier, IBC cells require low surface recombination velocity: when efficiencies over 22 % are targeted, the front surface recombination velocity needs to be below 30 cm/s[25].

Fig. 2a shows the minority carrier lifetimes of around 1 ms in our b-Si samples, which corresponds to a surface recombination velocity S_{eff} around 20 cm/s (see Fig. 2b.). These values are slightly higher than what we have reported before, and are probably caused by etching defects on the surface due to problems during the black silicon etching[17]. However, the values are still in the acceptable range from the solar cell point of view. In the reference samples the surface recombination velocities are as low as 3 cm/s.

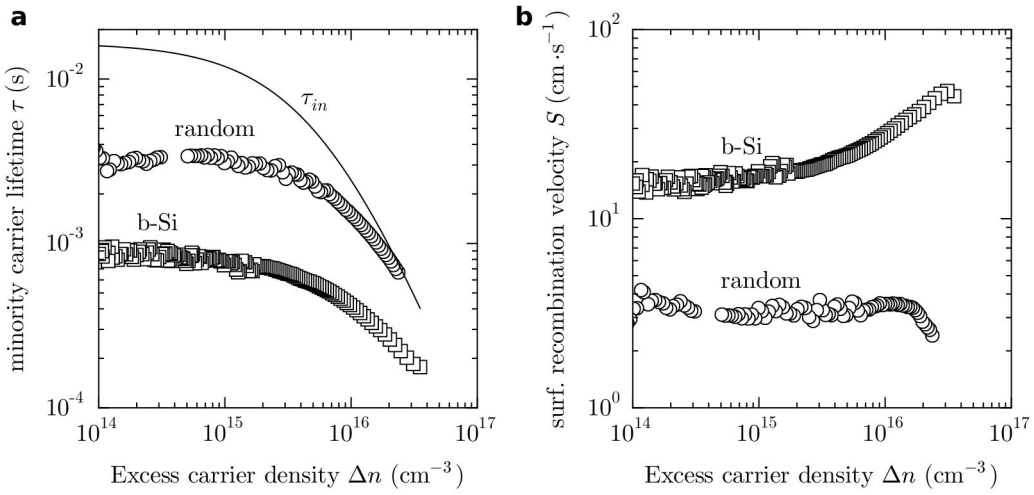

Figure 2. Lifetimes and corresponding surface recombination velocities. Minority carrier lifetimes (a) and the corresponding surface recombination velocities (b) as a function of the minority carrier density. Values for the b-Si sample are shown with squares whereas values for the random pyramid sample are shown with circles. The solid line in a) represents the intrinsic lifetime. Substrate resistivity was 2.6 ± 0.2 Ωcm in both samples.

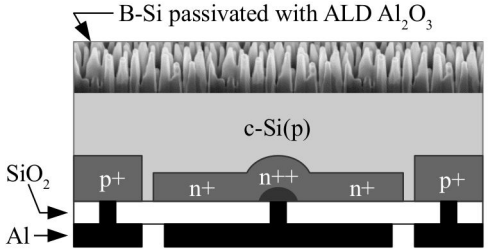

Figure 3. Structure of the IBC cell. A thin Al_2O_3 layer is deposited on the nanostructured front surface. The solar cell fabrication process is presented in the Methods section.

22.1% efficient black silicon solar cell

Figure 3 shows the cross-section of the IBC cell structure fabricated in this study. The collecting junction is on the back side while no contacts (and thus no shadowing) are present on the front side. The surface area of the cells is 9 cm^2. The cells introduce selective emitters, meaning that there is a heavily doped region just beneath the contact to reduce the contact resistance and to hide the highly recombining contact from the rest of the junction. Four different emitter coverages were applied: 67%, 75%, 80% and 86%. Identical solar cells but with random pyramid texture were fabricated as a reference. The details of the solar cell fabrication and characterization are described in the Methods section.

The current-voltage (*J-V)* and power-voltage (*P-V)* characteristics of the best black silicon solar cell are shown in Fig. 4a. These results were obtained for an emitter coverage of 80%. The photovoltaic parameter values are summarized in Table I, where the results are directly compared with its reference counterpart (cell with random pyramid texture). Measurements from the b-Si solar cell show efficiencies over 22.1% (independently confirmed at Fraunhofer ISE CalLab PV Cells testing laboratory), which is almost 4% absolute higher than values ever reached with any b-Si solar cell. In addition, this is the first time that the black silicon itself does not limit the solar cell efficiency since the efficiency is comparable to the reference counterpart cell.

The outstanding short circuit current density J_{sc} of 42.2 mA/cm^2 as well as the good open circuit voltage V_{oc} of 665 mV prove the excellent front surface passivation in the b-Si cell. This is clearly seen also from the external quantum efficiency (EQE) measurements in Fig. 4b that show a flat behaviour in the short wavelength range with a value around 96%. In fact, the main difference with the reference counterpart cell is on the short wavelength range, where the reference cell clearly exhibits lower EQE values. This can be attributed to the much lower reflectance of the b-Si in the UV range. The similar EQE values in the infrared region (λ=800—1200 nm) indicate near identical rear surfaces on both the b-Si and reference cells, as can be expected.

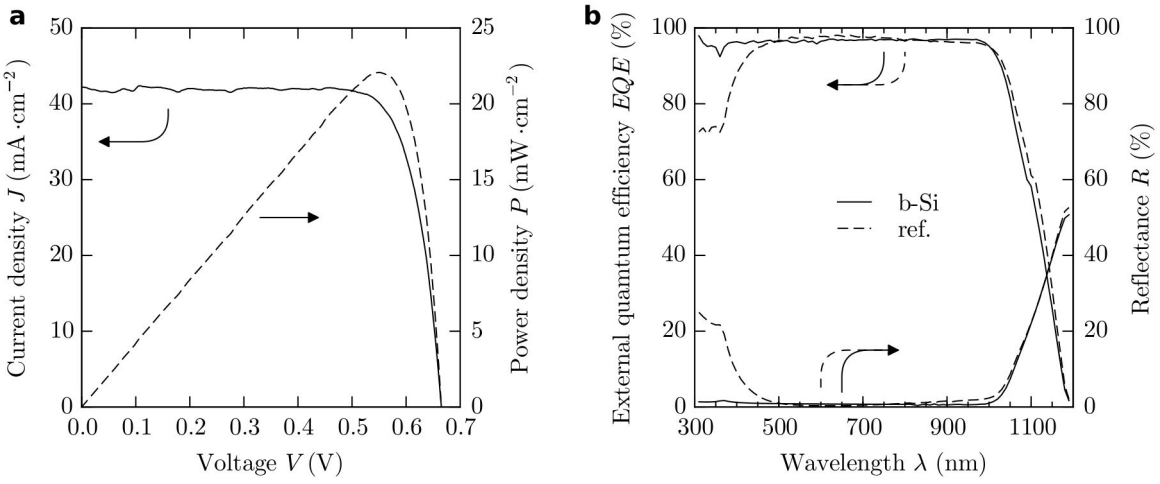

Figure 4. External quantum efficiency (EQE) and the *J-V* and *P-V* characteristics for the selected black silicon solar cell. a) The *J-V* (solid) and *P-V* (dashed) characteristics of the b-Si cell with 80% emitter coverage. b) EQE and reflectance measurements for the best b-Si (solid lines) and the corresponding randomly texturized (dashed lines) cell. EQE's were measured with 0.1 suns bias light.

Table I. Photovoltaic results of the black silicon solar cell and emitter coverage of 80%. As a comparison values from a random pyramid textured reference cell with the same emitter coverage.

Cell	J_{sc} (mA/cm^2)	V_{oc} (mV)	FF (%)	η (%)
Black silicon	**42.2**	**665**	**78.7**	**22.1**
Reference	42.0	667	78.6	22.0

Finally, due to the black silicon property of absorbing light with high acceptance angles, the high efficiency can be maintained independently of the direction of the incoming light (see Fig. 5a). This is not the case in the conventional antireflection coatings that are only optimized for the incident light perpendicular to the cell surface. This property has a high impact especially in photovoltaics, since the sun radiation impinges solar cells from different angles throughout the day and through the year. Fig. 5b shows the relative change in the photogenerated current with respect to normal illumination, for several incidence angles and considering both the reference and black cells. For the b-Si cell, changes in the photogenerated current are under 1% for incidence angles below 60º, whereas the reference counterpart loses up to nearly 4% in the same angle range. As a consequence, the quantity of energy delivered by the black silicon cell along the day/year also surpasses the energy produced by the reference solar cell. Fig. 5c shows a simulation of the relative increase in produced energy compared to the reference cell. For latitudes below 60º (Helsinki) relative increases greater than 2% are obtained over the year. This improvement is dependent on the season of the year. For instance, far from the equator, the increase is more important when insolation is lower (winter) and this asymmetry grows with the latitude. As it can be seen in fig 5d, at 40º of latitude the increase is more than 2.5% during the 4 months with less insolation. Details of the calculation procedure are given in the Methods section.

Our results show that the black silicon is no longer limiting the cell efficiency; thereby, further improvement should be possible by improving the cell structure. For example, even higher efficiencies could be expected by optimizing the emitter coverage. Other improvements could be implemented in the current IBC structures in order to increase fill factor (FF) and V_{oc} values. For instance, a thicker aluminium layer in fingers and busbars would reduce ohmic losses, thereby achieving higher FF values. Moreover, an optimized phosphorous doping profile in the low and high doped emitter regions might further decrease emitter saturation current density, J_{oe}, increasing Voc accordingly. Therefore, with realistic improved values of FF > 81% and Voc > 675 mV, and assuming the excellent J_{sc} (42.2 mA/cm^2) value reached in this study, efficiencies well beyond 23% are expected soon. Furthermore, since Al_2O_3 passivation has been reported to work on n-type surfaces as well,26 we plan to use the same approach reported here for n-type IBC structure, which has an even higher potential due to higher bulk minority carrier lifetimes.

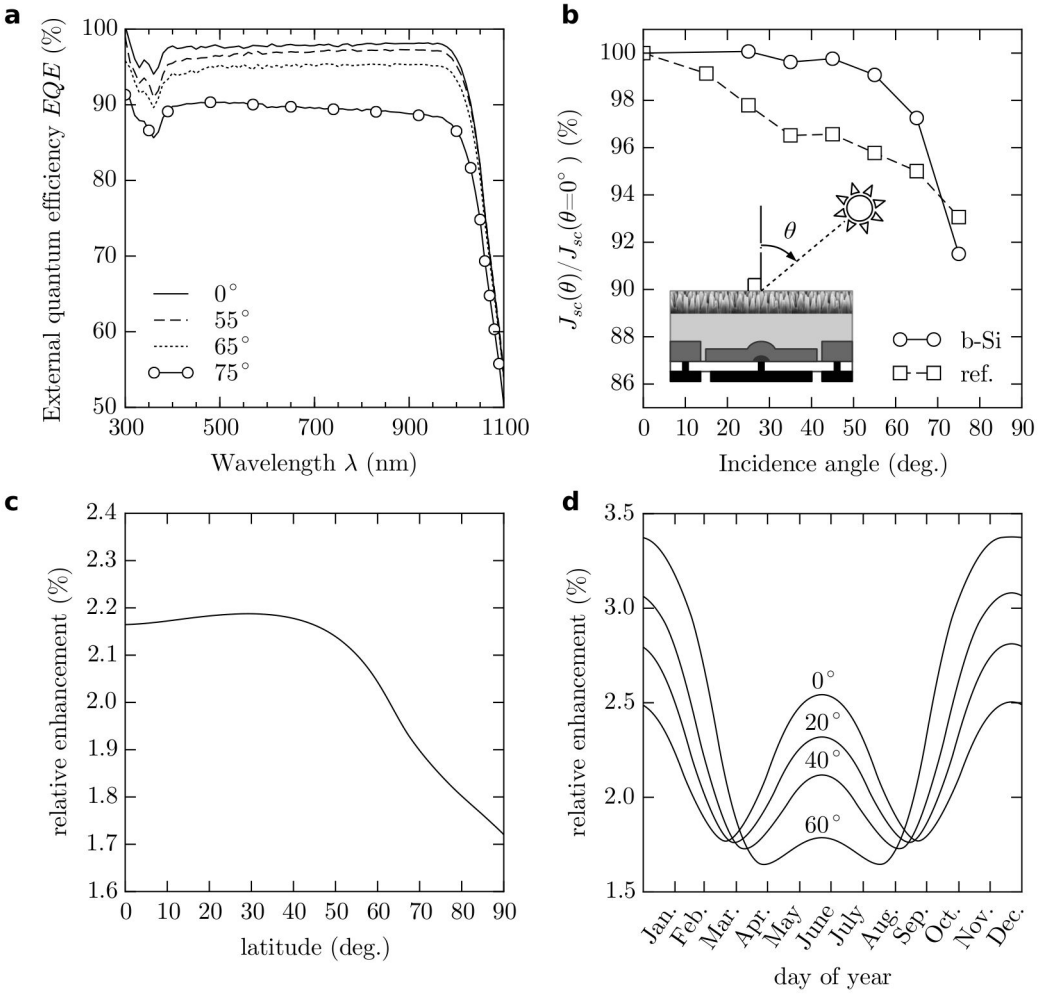

Figure 5. Angle dependent EQE and daily/yearly energy production enhancement. a) EQE of the b-Si cell for different angles of incidence. b) Relative photocurrent, with respect to photocurrent at normal incidence, for different light incidence angles for both the black silicon (circles) and the reference solar cells (squares). Light incidence angle is defined in the inset. c) Relative increase in total delivered energy along the year for the black silicon cell related to the reference cell as a function of the latitude and considering optimally tilted cells. d) Daily relative increase along the year of the energy generated by the black silicon cell compared to the reference cell for different locations (60º latitude corresponds to Helsinki, 40º to Barcelona).

In summary, we have successfully developed a high efficiency, p-type, b-Si IBC solar cell, with greater than 22 % efficiency with a surface area of 9.0 cm^2. In the record cell we can use its optimal surface reflectance without affecting surface recombination, due to the outstanding surface passivation achieved with conformal ALD Al_2O_3. Use of surface sensitive 280 μm thick IBC structure proves that the surface recombination, that has been hindering the utilization of b-Si in photovoltaics, is no longer a limiting factor. This should pave the way for even higher efficiencies in b-Si cells not only in IBC structures but also in existing and new solar cell concepts.

Methods

Sample fabrication. Black silicon was etched with a cryogenic inductively coupled plasma reactive-ion etching process (Plasmalab System 100, Oxford Instruments) at -120 ºC using SF_6 and O_2 as the etching gases. For the lifetime tests starting wafers were high quality 4 inch p-type Float Zone silicon <100> with a resistivity of 2.6 ± 0.2 Ωcm and thickness of 280 ± 20 µm. Some wafers were b-Si etched on both sides and the others were anisotropically etched using a mix of Tetramethylammonium hydroxide TMAH, isopropanol (IPA) and DI water (320 ml:350 ml:3300 ml) at 80ºC during 70 min to form random pyramids on both wafer surfaces. After the etching, the wafers were RCA cleaned and HF-dipped followed by surface passivation with 20 and 90 nm thick ALD Al_2O_3 in the b-Si etched and random textured samples respectively. ALD process was carried out in all cases using TMA as the aluminium source and H_2O as the oxidant. The surface passivation of the b-Si wafers was activated with a 30 minute anneal at 400 ºC in N_2. The random textured wafers were annealed using a forming gas atmosphere (95% N_2/5% H_2) at 400ºC during 10 min.

Black silicon IBC and reference solar cells with random pyramids were fabricated on high quality 4 inch p-type Float Zone silicon <100> with resistivity of 2.4 ± 0.2 Ωcm and thickness of 280 ± 20 µm. The main fabrication features are: i) boron and phosphorous diffusions using solid dopant sources to perform p+ (base contacts), n+ (low doped emitter) and n++ (high doped emitter) regions respectively which are patterned using standard photolithography ii) a black silicon (b-Si solar cells) or random textured (reference cells) surface passivated with 20 nm or 90 nm ALD Al_2O_3 films, respectively iii) a back reflector scheme consisting of a thermal SiO_2(110 nm)/Al(3 µm) stack. Al_2O_3 deposition on the b-Si cells was done using TMA and H_2O as the precursors and the passivation was activated with a 30 minute anneal at 400 ºC in N_2. The ALD process and annealing stage for the reference IBC cells were identical to the ones used for the reference lifetime samples described before. A total of 4 solar cells with different emitter coverage (i.e. the relative area of the emitter to the total rear surface area) 67%, 75%, 80% and 86% were fabricated on each wafer. Device areas (3 cm x 3 cm) were clearly defined by light windows through an e-beam evaporated aluminium metallization layer (0.4 µm thick) in the front side.

Sample characterization. Lifetimes as a function of minority carrier density of the symmetrically etched black silicon and random pyramid textured samples were measured with quasi steady state photoconductance method (Sinton Instruments WCT-120). The corresponding surface recombination velocities were calculated as described in the main text. Solar cells were measured using a solar simulator (ORIEL 94021A) under standard test conditions (AM1.5G 1 kW/m^2 solar spectrum T=25ºC). Only the nanostructured solar cell efficiency was independently confirmed by Fraunhofer ISE CalLab PV Cells certified photovoltaics testing laboratory. Calibration of the ORIEL simulator used may differ slightly. Reflectance measurements were carried out using a UV-vis-NIR spectrometer with an integrating sphere (Shimadzu 3600) in the 300-1200 nm wavelength range, whereas *EQE* characterization was performed using a solar cell quantum efficiency measurement system

(QEX10) with a beam spot area about 2 cm x 2 cm and 0.1 suns of bias light. Angle dependent *EQE* measurements were carried out with the same instrument but using and small beam light size (0.5 cm x 1 cm) in order to ensure that the whole light spot impinges into the active solar cell area.

Relative improvement calculation. We have calculated the relative improvement in performance among a black-silicon and a reference textured cell due to the different angles of incidence during the day and along the year. The calculation takes into account only direct sun radiation, while diffuse and albedo components are not considered. Calculations have been performed at different latitudes for a fixed flat panel optimally tilted for that particular latitude. A sun position algorithm[27] giving the sun vector at any time with an accuracy around 1º has been used. Local atmospheric effects are irrelevant as far as the calculation is restricted to relative improvements. Nevertheless, in the calculations we have estimated the irradiance on the Earth's surface along the year considering clear sky conditions and the air mass. Apparent solar dawn and dusk on the tilted plane of the PV module have been considered. In order to determine the output power, the short circuit current at a given time is scaled from the 1sun measured value taking into account the experimentally measured angle dependence. Finally, the maximum output power is determined and integrated in a daily and yearly basis.

References

[1] Clapham, P. B. & Hutley, M. C. Reduction of lens reflection by the “Moth eye” principle. *Nature* **3**, 281-282 (1973).

[2] Zhu J. *et al.* Optical Absorption Enhancement in Amorphous Silicon Nanowire and Nanocone Arrays. *Nano Lett.* **9** 279 (2008).

[3] Garnett, E & Yang, P. Light trapping in Silicon Nanowire Solar Cells. *Nano Lett.*, **10**, 1082-1087 (2010).

[4] Kelzenberg, M. D. *et al*., Enhanced absorption and carrier collection in Si wire arrays for photovoltaic applications. *Nature Materials* **9**, 239-244 (2010).

[5] Oh, J., Yuan, H.-C. & Branz, H. M. An 18.2%-efficient black-silicon solar cell achieved through control of carrier recombination in nanostructures. *Nature Nanotechnology* **7**, 743-748 (2012).

[6] Zhu, J., Hsu, C.-M., Yu, Z., Fan, S. & Cui, Y. Nanodome solar cells with efficient light management and self-cleaning. *Nanolett.* **10**, 1979-1984 (2010).

[7] de Boer, M. J. *et al*. Guidelines for etching silicon MEMS structures using fluorine high-density plasmas at cryogenic temperatures. *J. Micromech. Microeng.* **11**, 385-401 (2002).

[8] Gesemann, B., Wehrspohn, R., Hackner, A. & Müller, G. Large-scale fabrication of ordered silicon nanotip arrays used for gas ionization in ion mobility spectrometers. *IEEE Trans. Nanotechnol.* **10**, 50-52 (2011).

[9] Hoyer, P., Theuer, M., Beigang, R. & Kley, E.-B. Terahertz emission from black silicon. *Appl. Phys. Lett.* **93**, 091106 (2008).

[10] Sainiemi, L. *et al*. Rapid fabrication of high aspect ratio silicon nanopillars for chemical analysis. *Nanotechnology* **18**, 505303 (2007).

[11] Huang, Z. *et al*. Microstructured silicon photodetector. *Appl. Phys. Lett.* **89**, 033506 (2006).

[12] Ivanova, E. P. *et al*. Bactericidal activity of black silicon. *Nat. Commun.* **4**, 2838 (2013).

[13] Jeong, S., McGehee, M. D. & Cui, Y. All-back-contact ultra-thin silicon nanocone solar cells with 13.7% power conversion efficiency *Nature Communications* **4**, 2950, (2013).

[14] Zhong, S. *et al*. Influence of the texturing structure on the properties of black silicon solar cell. *Sol. Energ. Mat. Sol. C.* **108**, 200-204 (2013).

[15] Koynov, S., Brandt, M. S. & Stutzmann, M. Black multi-crystalline silicon solar cells. *Phys. Stat. Sol. RRL* **1**, R53-R55 (2007).

[16] Hoex, B., Schmidt, J., Pohl, P., van de Sanden, M. C. M. & Kessels, W. M. M. Silicon surface passivation by atomic layer deposition Al_2O_3. *J.Appl.Phys*. **104**, 044903 (2008).

[17] Repo, P. *et al*. Effective passivation of black silicon surfaces by atomic layer deposition. *IEEE J. Photovolt.* **3**, 90-94 (2013).

[18] Otto, M. *et al*, Extremely low surface recombination velocities in black silicon passivated by atomic layer deposition. *Appl. Phys. Lett* **100**, 191603 (2012).

[19] Neuhaus, D. & Münzer, A. Industrial silicon wafer solar cells. *Advances in OptoElectronics*, **2007**, Article ID 24521 (2007).

[20] Halbwax, M. *et al*. Micro and nano-structuration of silicon by femtosecond laser: Application to silicon photovoltaic cells fabrication. *Thin Solid Films* **516**, 6791-6795 (2008).

[21] Toor, F., Branz, H. M., Page, M. R., Jones, K. M. & Yuan, H.-C. Multi-scale surface texture to improve blue response of nanoporous black silicon solar cells. *Appl. Phys. Lett*. **99**, 103501 (2011).

[22] Sainiemi L. *et al*. Non-reflecting silicon and polymer surfaces by plasma etching and replication. *Adv. Mater.* **23**, 122-126 (2011).

[23] Huang Y.-F. *et al*. Improved broadband and quasi-omnidirectional anti-reflection properties with biomimetic silicon nanostructures. *Nature Nanotechnology* **2**, 770-774 (2007).

[24] Richter, A., Glunz, S. W., Werner, F., Schmidt, J. & Cuevas, A. Improved quantitative description of Auger recombination in crystalline silicon. *Phys. Rev. B* **86**, 165202 (2012).

[25] Carrio, D. *et al*. Rear contact optimization based on 3D simulations for IBC solar cells with point-like doped contacts. *Energy Procedia* **55** 47 (2014).

[26] Hoex, B., van de Sanden, M. C. M., Schmidt, J., Brendel, R. & Kessels, W. M. M. Surface passivation of phosphorus-diffused n+-type emitters by plasma-assisted atomic-layer deposited Al_2O_3. *Phys. Stat. Sol. RRL* **6**, 4-6 (2012).

[27] Masters, G. M. Renewable and Efficient Electric Power Systems, John Wiley & Sons, New York, NY, USA, 2004.

Acknowledgements

This work has been supported by the network 'Nanophotonics for Energy Efficiency' Grant agreement 248855, Effinano-project funded by the School of Electrical Engineering at Aalto University as well as Tekes-funded project PASSI. Authors also acknowledge The Centre for Research in NanoEngineering CRnE and Aalto University Micronova Nanofabrication Centre for providing the facilities. Dr. Trifon Trifonov is acknowledged for his help and comments to perform reflectance measurements and Ville Vähänissi for providing valuable comments regarding the manuscript writing.

Author contributions

H.S. and R.A. conceived and designed the experiments: P.R. G.G. P.O. and E.C. performed the experiments: P.O. analyzed the data: M. G. performed the angle-dependent simulations. H.S. wrote the paper. All authors discussed the results and commented on the manuscript.

Additional information

Supplementary information accompanies this paper at www.nature.com/naturenanotechnology. Reprints and permission information is available online at http://npg.nature.com/reprintsandpermissions/. Correspondence and requests for materials should be addressed to H.S.